possibly contributing to the chronic, recurrent inflammation in these skin conditions (Wang, 2015). Thus, PG may be part of the autoinflammatory spectrum, together with HS and acne.

Genetic studies have identified 21 distinct mutations in *NCSTN*, most of them associated with HS/acne inversa (Li et al., 2011; Liu et al., 2011; Nomura et al., 2013; Pink et al., 2011; Wang et al., 2010; Zhang et al., 2013). To the best of our knowledge, the pathogenic variant identified in this study, c.1635C>G (p.Tyr545*) in *NCSTN*, is previously unreported, providing strong evidence for the critical functional role of *NCSTN* in the phenotype of our patients.

CONFLICT OF INTEREST

The authors state no conflict of interest.

ACKNOWLEDGMENTS

We thank the families for their participation in this study. Carol Kelly assisted in manuscript preparation.

Mehrshid Faraji Zonooz[1,9], Farahnaz Sabbagh-Kermani[2,9], Zohreh Fattahi[1,3], Mahsa Fadaee[1,3], Mohammad Reza Akbari[4,5], Rezvan Amiri[6], Hassan Vahidnezhad[7,8], Jouni Uitto[8], Hossein Najmabadi[1,3] and Ariana Kariminejad[1,*]

[1]Kariminejad-Najmabadi Pathology and Genetics Center, Tehran, Iran; [2]Clinical Research Unit, Afzalipoor Hospital, Kerman University of Medical Sciences, Kerman, Iran; [3]Genetics Research Center, University of Social Welfare and Rehabilitation Sciences, Tehran, Iran; [4]Dalla Lana School of Public Health, University of Toronto, Toronto, Canada; [5]Women's College Research Institute, University of Toronto, Toronto, Canada; [6]Leishmaniasis Research Center, Kerman University of Medical Sciences, Kerman, Iran; [7]Biotechnology Research Center, Department of Molecular Medicine, Pasteur Institute of Iran, Tehran, Iran; and [8]Department of Dermatology and Cutaneous Biology, Thomas Jefferson University, Philadelphia, Pennsylvania, USA

[9]These authors contributed equally to this work.

**Corresponding author e-mail: arianakariminejad@yahoo.com*

SUPPLEMENTARY MATERIAL

Supplementary material is linked to the online version of the paper at www.jidonline.org, and at http://dx.doi.org/10.1016/j.jid.2016.02.801.

REFERENCES

Braun-Falco M, Kovnerystyy O, Lohse P, Ruzicka T. Pyoderma gangrenosum, acne, and suppurative hidradenitis (PASH)—a new autoinflammatory syndrome distinct from PAPA syndrome. J Am Acad Dermatol 2012;66:409–15.

Duchatelet S, Miskinyte S, Join-Lambert O, Ungeheuer MN, Frances C, Nassif A, et al. First nicastrin mutation in PASH (pyoderma gangrenosum, acne and suppurative hidradenitis) syndrome. Br J Dermatol 2015;173:610–2.

Ingram JR, Piguet V. Phenotypic heterogeneity in hidradenitis suppurativa (acne inversa): classification is an essential step toward personalized therapy. J Invest Dermatol 2013;133:1453–6.

Li CR, Jiang MJ, Shen DB, Xu HX, Wang HS, Yao X, et al. Two novel mutations of the nicastrin gene in Chinese patients with acne inversa. Br J Dermatol 2011;165:415–8.

Liu Y, Gao M, Lv YM, Yang X, Ren YQ, Jiang T, et al. Confirmation by exome sequencing of the pathogenic role of NCSTN mutations in acne inversa (hidradenitis suppurativa). J Invest Dermatol 2011;131:1570–2.

Lu P, Bai XC, Ma D, Xie T, Yan C, Sun L, et al. Three-dimensional structure of human gamma-secretase. Nature 2014;512:166–70.

Miskinyte S, Nassif A, Merabtene F, Ungeheuer MN, Join-Lambert O, Jais JP, et al. Nicastrin mutations in French families with hidradenitis suppurativa. J Invest Dermatol 2012;132:1728–30.

Nomura Y, Nomura T, Sakai K, Sasaki K, Ohguchi Y, Mizuno O, et al. A novel splice site mutation in NCSTN underlies a Japanese family with hidradenitis suppurativa. Br J Dermatol 2013;168:206–9.

Pan Y, Lin MH, Tian X, Cheng HT, Gridley T, Shen J, et al. Gamma-secretase functions through Notch signaling to maintain skin appendages but is not required for their patterning or initial morphogenesis. Dev Cell 2004;7:731–43.

Pink AE, Simpson MA, Brice GW, Smith CH, Desai N, Mortimer PS, et al. PSENEN and NCSTN mutations in familial hidradenitis suppurativa (Acne Inversa). J Invest Dermatol 2011;131:1568–70.

Pink AE, Simpson MA, Desai N, Trembath RC, Barker JN. γ-Secretase mutations in hidradenitis suppurativa: new insights into disease pathogenesis. J Invest Dermatol 2013;133:601–7.

Wang B. γ-Secretase mutation and consequently immune reaction involved in pathogenesis of acne inversa. J Invest Dermatol Symp Proc 2015;17:25.

Wang B, Yang W, Wen W, Sun J, Su B, Liu B, et al. γ-Secretase gene mutations in familial acne inversa. Science 2010;330:1065.

Wise CA, Gillum JD, Seidman CE, Lindor NM, Veile R, Bashiardes S, et al. Mutations in CD2BP1 disrupt binding to PTP PEST and are responsible for PAPA syndrome, an autoinflammatory disorder. Hum Mol Genet 2002;11:961–9.

Zhang C, Wang L, Chen L, Ren W, Mei A, Chen X, et al. Two novel mutations of the NCSTN gene in Chinese familial acne inverse. J Eur Acad Dermatol Venereol 2013;27:1571–4.

IL-13 Signals Independent of IL-4 Receptor-Alpha Chain to Drive Ovalbumin-Induced Dermatitis

Journal of Investigative Dermatology (2016) **136,** 1286–1290; doi:10.1016/j.jid.2015.11.033

TO THE EDITOR

Atopic dermatitis (AD) is an allergic skin condition that can result from intrinsic genetic factors or repetitive occupational damage. Disruption of the skin barrier leads to sensitization to allergens followed by local inflammation (Leung et al., 2004; Pigatto et al., 1992). Strong evidence has shown that the T helper-2 (Th2) cytokine, IL-13, is the dominant disease-causing factor in the pathogenesis of AD in mice (Nieuwenhuizen et al., 2009; Sivaprasad et al., 2010; Tazawa et al., 2004). Hence, it is possible that patients with AD would benefit from

Abbreviations: AD, atopic dermatitis; ERK, extracellular signal-regulated kinase; MAPK, mitogen-activated protein kinase; OVA, ovalbumin; PBS, phosphate buffered saline; Rα, receptor-alpha; Th2, T helper 2; TGF, transforming growth factor

Accepted manuscript published online 16 February 2016; corrected proof published online 15 April 2016

© 2016 The Authors. Published by Elsevier, Inc. on behalf of the Society for Investigative Dermatology.

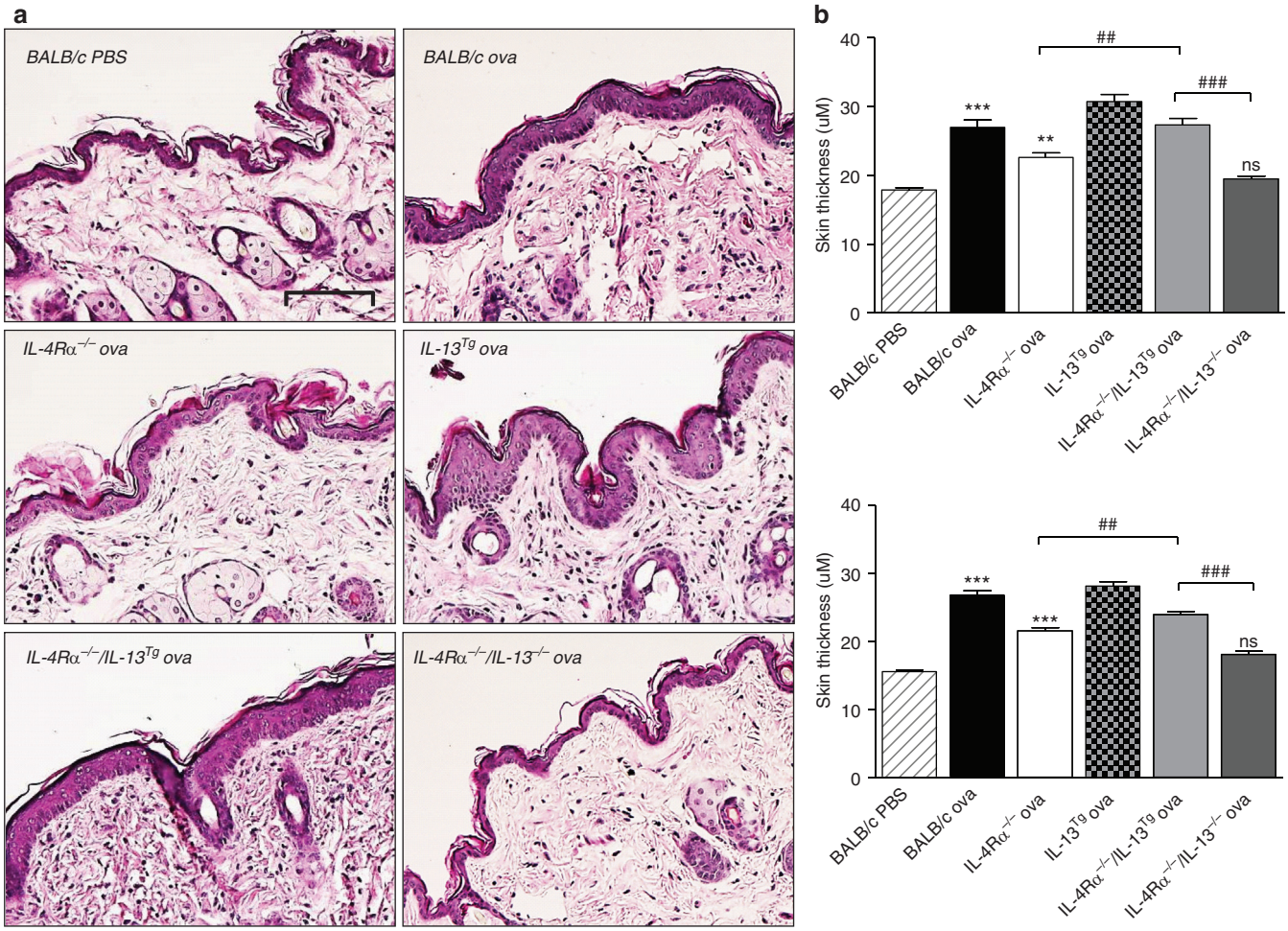

Figure 1. IL-13 causes dermatitis in IL-4Rα—deficient mice. **(a)** Hematoxylin and eosin stained skin sections. Original magnification ×200. **(b)** Epidermal thickness from two individual experiments. Data represent at least 2 individual experiments (n = 5–6). $^{**}P < 0.01$, $^{***}P < 0.001$ versus BALB/c PBS-treated mice; $^{\#\#}P < 0.01$, $^{\#\#\#}P < 0.001$ for IL-4Rα$^{-/-}$ OVA versus IL-4Rα$^{-/-}$/IL-13$^{-/-}$ or IL-4Rα$^{-/-}$/IL-13^{Tg} OVA mice or IL-4Rα$^{-/-}$/IL-13$^{-/-}$ versus IL-4Rα$^{-/-}$/IL-13^{Tg} mice. Scale bar = 100 μm. Values are given as mean ± standard error of the mean, and significant differences were determined using unpaired two-tailed Student *t* tests (GraphPad Prism version 4, GraphPad Software, San Diego, CA). $P < 0.05$ was considered significant. IL-4Rα, IL-4 receptor-alpha; ns, not significant; OVA, ovalbumin; PBS, phosphate buffered saline.

treatments specifically targeting IL-13 signaling pathways. However, current treatment strategies are limited to broader therapies, such as emollients, topical glucocorticoids, and calcineurin inhibitors (Beck et al., 2014; De Benedetto et al., 2012; Gittler et al., 2012). A recent study by Beck et al. (2014), which used the monoclonal antibody dupilumab to block IL-4 receptor-alpha (IL-4Rα) signaling, showed promise in targeting specific immunological pathways. Until recently, IL-13 was thought to signal only through the IL-4Rα/IL-13Rα1 complex; however, recent data suggest that IL-13 may also signal via IL-13Rα2, previously known as a decoy receptor. In AD, the signaling pathway of IL-13 remains to be defined. In this study we addressed this problem by using a combination of IL-4Rα—deficient mice that lacked or overexpressed IL-13 to determine if IL-13 can signal independently of the IL-4Rα chain to mediate AD. Our results may have potential implications for therapeutic strategies, such as using IL-4Rα—antagonists to treat the disease.

Ovalbumin (OVA)-induced dermatitis is a classic murine model of AD in which repeated epicutaneous application of OVA results in local skin inflammation and systemic sensitization. This reflects what is seen in human disease, where levels of associated Th2 cytokines are increased, specifically IL-4, IL-13, and IL-5 (Brandt and Sivaprasad, 2011; Jin et al., 2009). In mice IL-13 mediates local skin pathology (Nieuwenhuizen et al., 2009), and in humans IL-13 mRNA is increased and associated with AD (Hamid et al., 1996; Tazawa et al., 2004). Differences in responses driven by IL-4 or IL-13 can be attributed to differing signaling pathways. Both IL-4 and IL-13 can signal via the IL-4Rα chain, which can associate either with the common gamma chain (type I) to form IL-4 receptor type 1, through which only IL-4 can signal, or with the IL-13Rα1 (type II) subunit to form the IL-13 receptor type 1 chain, through which both IL-4 and IL-13 can signal (Nelms et al., 1999). In a previous study we found that IL-13 was responsible for the induction of skin pathology in *Anisakis* species-induced dermatitis, because IL-13$^{-/-}$ but not IL-4$^{-/-}$ mice were protected from disease (Nieuwenhuizen et al., 2009).

Furthermore, abrogation of IL-4Rα signaling significantly reduced epidermal

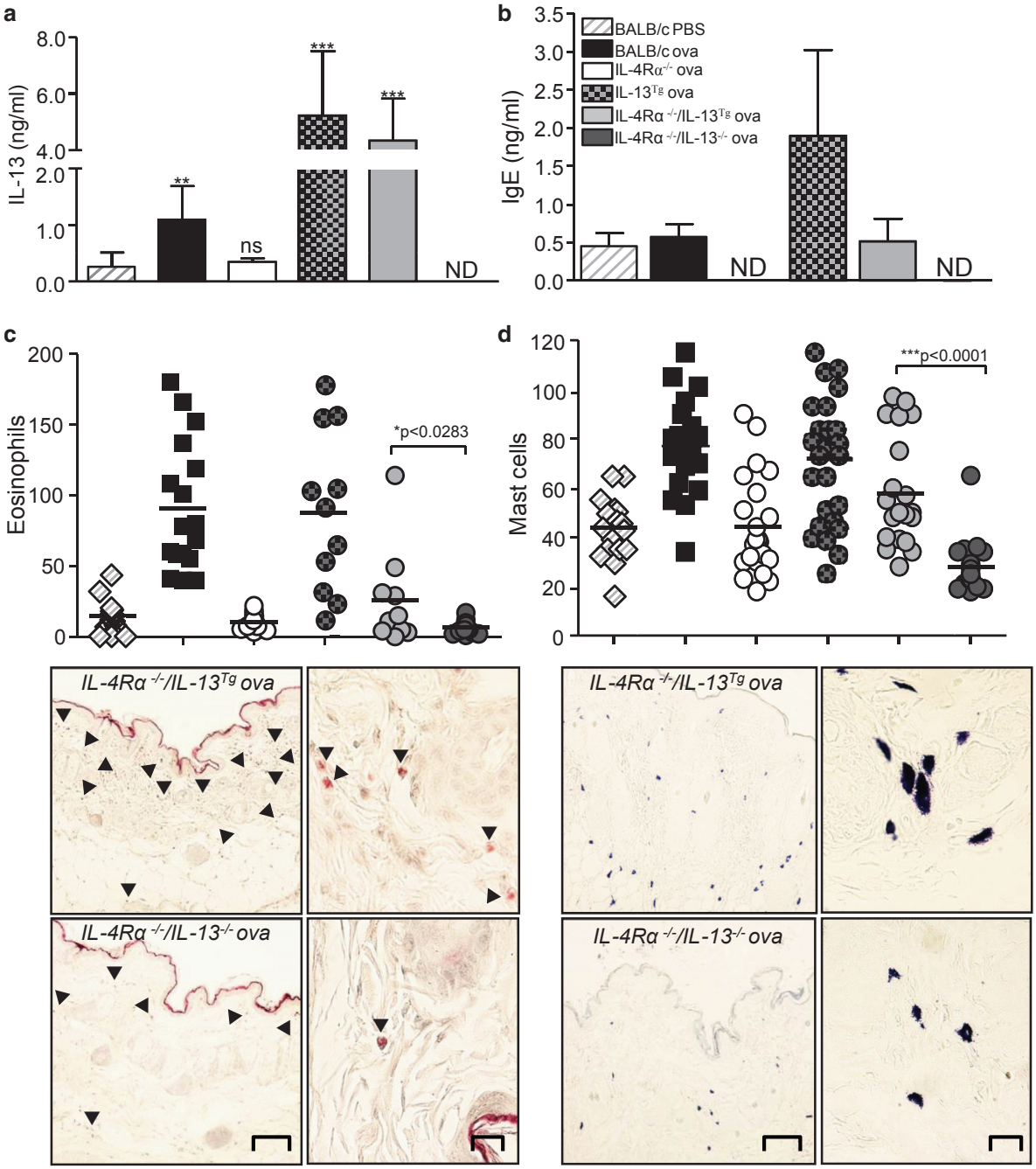

Figure 2. IL-13 is important in inducing the allergic phenotype during dermatitis. (a) IL-13 production in lymph nodes. **(b)** Total serum IgE level. Cell infiltration into the skin showing **(c)** eosinophils and **(d)** mast cells (including histology). Data represent 2 or more individual experiments (n = 5–6). $^{**}P < 0.01$ and $^{***}P < 0.001$ versus BALB/c PBS-treated mice. **(c)** and **(d)** represent pooled data from 2 independent experiments, * and *** represent IL-4Rα$^{-/-}$/IL-13$^{-/-}$ vs. IL-4Rα$^{-/-}$/IL-13^{Tg}. Scale bar left panel = 100 μm and scale bar right panel = 20 μm. Values are given as mean ± standard error of the mean, and significant differences were determined using unpaired two-tailed Student *t* tests (GraphPad Prism version 4, GraphPad Software, San Diego, CA). Values of $p < 0.05$ were considered significant. IL-4Rα, IL-4 receptor-alpha; ND, not determined; ns, not significant; ova, ovalbumin; PBS, phosphate buffered saline.

hyperplasia and skin inflammation compared with wild type mice (Nieuwenhuizen et al., 2009). An important role for IL-4Rα in AD was recently confirmed in a clinical study, in which treatment with the anti—IL-4Rα antibody dupilumab significantly improved signs and symptoms of AD (Beck et al., 2014). Because recent evidence suggests that IL-13 could signal independently of IL-4Rα (Brunner et al., 2013; Fichtner-Feigl et al., 2006), which could have important implications for therapeutic intervention, we aimed to determine whether IL-4Rα—independent IL-13 signaling is important in AD. Using a genetic loss or gain strategy, we compared double-deficient IL-4Rα$^{-/-}$/IL-13$^{-/-}$ mice with IL-R4α—deficient, IL-13—overexpressing (IL-4Rα$^{-/-}$/IL-13^{Tg}) mice on a BALB/c background. This allowed us to detect the role of IL-13 in the presence or absence of the IL-4Rα chain during OVA-induced AD. All mice were housed in specific pathogen-free conditions at the University of Cape Town, South Africa, and experiments

were approved by the University's Animal Ethics Committee.

Our results showed that although mice deficient in IL-4Rα still showed significant epidermal hyperplasia compared with phosphate buffered saline (PBS)-treated control mice, IL-4Rα$^{-/-}$/IL-13$^{-/-}$ mice were completely protected (Figure 1a and b), indicating that IL-13 was responsible for the partial protection of IL-4Rα$^{-/-}$ mice. This was confirmed by the fact that overexpressing IL-13 in IL-4Rα$^{-/-}$ mice (IL-4Rα$^{-/-}$/IL-13^{Tg}) resulted in more severe dermatitis, with increased epidermal hyperplasia and dermal inflammation, compared with IL-4Rα$^{-/-}$ mice (Figure 1a and b). In the absence of IL-4Rα, IL-13 levels were low but still present, and IgE levels were not detectable (Figure 2a and b). However, IL-4Rα$^{-/-}$/IL-13^{Tg} mice had significantly raised levels of IL-13, which were accompanied by an increase in IgE, compared with IL-4Rα$^{-/-}$ mice. Although eosinophil infiltration appeared to be controlled by IL-4Rα (Figure 2c), IL-13 appeared to partially regulate mast cell infiltration, because significantly more mast cells were recruited in IL-4Rα$^{-/-}$/IL-13^{Tg} mice than in IL-4Rα$^{-/-}$/IL-13$^{-/-}$ mice (Figure 2d). PBS-treated controls of all genetically altered mouse strains showed no difference in cell infiltration or epidermal thickening compared with wild type PBS-treated mice (data not shown). These results strongly suggest that IL-13 is responsible for OVA-induced dermatitis independent of the IL-4Rα chain, which may mediate dermatitis partially by regulating levels of Th2 cytokines, including IL-13.

Alternative signaling pathways for IL-13 remain to be elucidated in dermatitis and could include signaling via IL-13Rα2, previously believed to be only a decoy receptor for IL-13. Despite conflicting reports regarding the functions of IL-13Rα2, increasing evidence suggests that IL-13Rα2 may be a signaling receptor for IL-13, because an independent IL-13/IL-13Rα2 signaling pathway was found that can control activation of activator protein-1 (AP-1) to induce transforming growth factor-β secretion (Brunner et al., 2013; Fichtner-Feigl et al., 2006). It has further been shown that IL-13 binding to IL-13Rα2 mediates initiation of mitogen-activated protein kinase (MAPK) (extracellular signal-regulated kinase [ERK]) signaling (Mandal and Levine, 2010). Sustained ERK phosphorylation was observed in the sensory neurons of mice with allergic contact dermatitis (Zhao et al., 2013). In the chronic itch model described in this study, inhibition of BRAF (a serine/threonine kinase that activates ERK) signaling attenuated itch sensations, suggesting Raf—MAPK/ERK kinase—ERK signaling as a key regulator in initiating and maintaining chronic itch. Our preliminary data showed significantly increased ERK1 and ERK2 phosphorylation in the skin of OVA-treated IL-4Rα$^{-/-}$/IL-13^{Tg} mice compared with IL-4Rα$^{-/-}$/IL-13$^{-/-}$ mice (see Supplementary Figure S1 online). This is consistent with the previously described role of IL-13Rα in MAPK signaling (Mandal and Levine, 2010), but further evidence is required before conclusions can be drawn about the mechanisms of IL-4Rα—independent IL-13 signaling. Currently we are generating IL-13Rα2 floxed mice to investigate the contribution of IL-13/IL-13Rα2 signaling to dermatitis pathology.

In summary, we showed that IL-13 is able to signal independent of the IL-4Rα chain in AD, which may lead to the identification of molecular pathways downstream of IL-13 signaling that could be targeted in future therapies for AD. IL-13 overexpression in the absence of IL-4Rα reconstituted the disease phenotype and resulted in phosphorylation of ERK1 and ERK2. The role of IL-4Rα—independent signaling of IL-13 is an important consideration for therapies that neutralize IL-4Rα in the treatment of allergic diseases, because it is possible that combined neutralization of IL-4Rα and IL-13 may be more effective.

CONFLICT OF INTEREST

The authors state no conflict of interest.

ACKNOWLEDGMENTS

The authors would like to thank Lizette Fick, Marilyn Tyler, Zoe Lotz, Wendy Green, and Rayaana Fredericks for technical assistance and Dr. Reece Marillier and Josipa Raguz for discussion. This work was supported by the National Research Foundation (NRF, South Africa), the South African Research Chair Initiative (SARChI), and the South African Medical Research Council (SAMRC). JCH is a recipient of the Naledi Pandor NRF postdoctoral fellowship and Deutscher Akademischer Austausch Dienst (DAAD).

J. Claire Hoving[1,2,4], Natalie E. Nieuwenhuizen[1,2,4,5], Georgia Schäfer[3], Arieh A. Katz[3] and Frank Brombacher[1,2,*]

[1]*International Centre for Genetic Engineering and Biotechnology (ICGEB), Cape Town, South Africa, component;* [2]*Institute of Infectious Disease and Molecular Medicine (IDM), Division of Immunology, Faculty of Health Sciences, University of Cape Town, Cape Town, South Africa; and* [3]*Division of Medical Biochemistry and the Institute of Infectious Diseases and Molecular Medicine, Faculty of Health Sciences, University of Cape Town, Cape Town, South Africa*
[4]*These authors contributed equally to this work.*
[5]*Current address: Department of Immunology, Max Planck Institute for Infection Biology, Chariteplatz 1, Berlin, Germany*
[*]*Corresponding author e-mail: frank.brombacher@icgeb.org*

SUPPLEMENTARY MATERIAL

Supplementary material is linked to the online version of the paper at www.jidonline.org, and at http://dx.doi.org/10.1016/j.jid.2015.11.033

REFERENCES

Beck LA, Thaçi D, Hamilton JD, Graham NM, Bieber T, Rocklin R. Dupilumab treatment in adults with moderate-to-severe atopic dermatitis. N Engl J Med 2014;10:130—9.

Brandt E, Sivaprasad U. Th2 cytokines and atopic dermatitis. J Clin Cell Immunol 2011;2:110.

Brunner SM, Schiechl G, Kesselring R, Martin M, Balam S, Schlitt HJ. IL-13 signalling via IL-13Rα2 triggers TGF-β1-dependent allograft fibrosis. Transplant Res 2013;2:16.

De Benedetto A, Kubo A, Beck LA. Skin barrier disruption: a requirement for allergen sensitization? J Invest Dermatol 2012;132:949—63.

Fichtner-Feigl S, Strober W, Kawakami K, Puri RK, Kitani A. IL-13 signalling through the IL-13alpha2 receptor is involved in induction of TGF-beta1 production and fibrosis. Nat Med 2006;12:99—106.

Gittler JK, Shemer A, Suarez-Farinas M, Fuentes-Duculan J, Gulewicz KJ, Wang CQ. Progressive activation of T(H)2/T(H)22 cytokines and selective epidermal proteins characterizes acute and chronic atopic dermatitis. J Allergy Clin Immunol 2012;130:1344—54.

Hamid Q, Naseer T, Minshall EM, Song YL, Boguniewicz M, Leung DY. In vivo expression of IL-12 and IL-13 in atopic dermatitis. J Allergy Clin Immunol 1996;98:225—31.

Jin H, He R, Oyoshi M, Geha RS. Animal models of atopic dermatitis. J Invest Dermatol 2009;129:31—40.

Leung DY, Boguniewicz M, Howell MD, Nomura I, Hamid QA. New insights into atopic dermatitis. J Clin Invest 2004;113:651—7.

Mandal D, Levine A. Elevated IL-13Rα2 in intestinal epithelial cells from ulcerative colitis or colorectal cancer initiates MAPK pathway. Inflamm Bowel Dis 2010;16:753—64.

Nelms K, Keegan AD, Zamorano J, Ryan JJ, Paul WE. The IL-4 receptor: signaling mechanisms and biologic functions. Annu Rev Immunol 1999;17:701–38.

Nieuwenhuizen N, Herbert DR, Brombacher F, Lopata AL. Differential requirements for interleukin (IL)-4 and IL-13 in protein contact dermatitis induced by Anisakis. Allergy 2009;64:1309–18.

Pigatto PD, Legori A, Bigardi AS. Occupational dermatitis from physical causes. Clin Dermatol 1992;10:231–43.

Sivaprasad U, Warrier MR, Gibson AM, Chen W, Tabata Y, Bass SA. IL-13Rα2 has a protective role in a mouse model of cutaneous inflammation. J Immunol 2010;185:6802–8.

Tazawa T, Sugiura H, Sugiura Y, Uehara M. Relative importance of IL-4 and IL-13 in lesional skin of atopic dermatitis. Arch Dermatol Res 2004;295:459–64.

Zhao Z, Huo F, Jeffry J, Hampton L, Demehri S, Kim S. Chronic itch development in sensory neurons requires BRAF signalling pathways. J Clin Invest 2013;123:4769–80.

The Alarmin IL-33 Derived from HSV-2-Infected Keratinocytes Triggers Mast Cell-Mediated Antiviral Innate Immunity

Journal of Investigative Dermatology (2016) **136,** 1290–1292; doi:10.1016/j.jid.2016.01.030

TO THE EDITOR

IL-33, a member of the IL-1 family, is a nuclear-associated multifunctional cytokine that acts as damage-associated molecular patterns, so-called "alarmins," following external insults to induce innate immunity, inflammation, and allergy (Cayrol and Girard, 2014; Molofsky et al., 2015). IL-33 interacts with the IL-1 family receptor ST2, which is expressed on mast cells (MCs), eosinophils, basophils, natural killer cells, group 2 innate lymphoid cells, and T cells (Cayrol and Girard, 2014). Although IL-33 is most frequently characterized as an epithelial cytokine that promotes T helper type 2-mediated immune responses, recent studies have extended its biology to include roles in basal tissue regulation, organ-specific injury and repair, T helper type 1-, T helper type 17-, or cytotoxic T lymphocyte-mediated immune responses, and immune tolerance by affecting regulatory T cells (Gajardo Carrasco et al., 2015; Molofsky et al., 2015). Moreover, IL-33/ST2 signaling has been recently found to be involved in the response to viral infections (Rostan et al., 2015), such as airway infection with influenza virus or parainfluenza virus (Byers et al., 2013; Chang et al., 2011; Monticelli et al., 2011), splenic infection with lymphocytic choriomeningitis virus (Baumann et al., 2015; Bonilla et al., 2012), and intraperitoneal infection with mouse cytomegalovirus (Nabekura et al., 2015). Some of these studies have highlighted the new role of IL-33 as an "alarmin" in host defense against viral infections; however, its role against cutaneous viral infections remains to be defined.

Herpes simplex virus type 2 (HSV-2) is a sexually transmitted pathogen that infects more than 500 million people worldwide and causes most cases of genital herpes (Looker et al., 2008). Although adaptive immune responses mediated by HSV-specific cytotoxic T lymphocytes are known to play a central role in controlling primary and recurrent HSV infections, the importance of innate immune effectors, including plasmacytoid dendritic cells, natural killer cells, and γδ T lymphocytes, has been recently re-emphasized, either in direct immune control or via modulation of adaptive immune responses (Chew et al., 2009; Kawamura et al., 2014). In addition to these innate immune cells, we have recently demonstrated that MCs are critically involved in host defense at HSV-infected sites through tumor necrosis factor-α and IL-6 production (Aoki et al., 2013). Our study also demonstrated that IL-33 expression was upregulated by HSV-infected Pam-212 keratinocytes in vitro, suggesting the significance of IL-33 as a trigger for the host anti-HSV innate immunity.

To further explore cutaneous IL-33 expression after HSV-2 infection in vivo, we examined the tissue levels of IL-33 in an HSV-2 cutaneous infection model, whereby HSV-2 was intradermally injected into wild-type (WT) mice. As expected, significant IL-33 production was observed at the skin sites of infection, which peaked at 1 day after infection, and importantly, paralleled the kinetics of HSV-2 titer in the skin (Figure 1a, Detailed methods; see Supplementary Materials online), suggesting that productive viral replication promotes IL-33 release in the murine skin. Immunohistochemical staining for IL-33 in HSV-2-infected skin at 1 day after infection revealed that IL-33 was dominantly expressed in the nucleus of epidermal keratinocytes (Figure 1b). Importantly, we could confirm a significant increase in IL-33 expression and production by HSV-2-infected human HaCaT keratinocytes and normal human epidermal keratinocytes (Supplementary Figures S1 and S2 online). We found that increased IL-33 expression was selectively detected on damaged or degenerating HaCaT cells and normal human epidermal keratinocytes 24 hours after HSV-2 exposure, and the frequency of IL-33-expressing cells was increased in a multiplicity of infection-dependent manner. In line with these findings, we could detect abundant IL-33 expression in degenerating keratinocytes in lesional blister roof of HSV-infected patients (Supplementary Figure S3 online). All patients provided written informed consent to participate in the study, which was

Abbreviations: BMMC, bone marrow-derived mast cell; HSV-2, herpes simplex virus-2; MC, mast cell; WT, wild-type

Accepted manuscript published online 9 February 2016; corrected proof published online 21 March 2016

© 2016 The Authors. Published by Elsevier, Inc. on behalf of the Society for Investigative Dermatology.

Supplementary: Methods

Mice

All transgenic mouse strain used were either generated in BALB/c embryonic stem cells, or backcrossed at least 9 generations to BALB/c. Male BALB/c mice (6-8 weeks old) and IL-4$^{-/-}$, IL-13$^{-/-}$, IL-4Rα$^{-/-}$ and IL-13 transgenic [IL-13^{Tg}] mice on a BALB/c background were used in the experiments (Mckenzie et al, 1998; Podolsky et al, 2002, Noben-trauth et al, 1996; Mohrs et al, 1999; Emson et al, 1998). Furthermore, IL-4$^{-/-}$, IL-13$^{-/-}$, IL-4Rα$^{-/-}$ and IL-13^{Tg} mice were intercrossed to generate IL-4/IL-13, IL-4Rα/IL-4, IL-4Rα/IL-13 double-deficient and IL-4Rα$^{-/-}$/IL-13^{Tg} strains. All mice were housed in specific pathogen-free conditions at the University of Cape Town, South Africa and experiments were approved by the University's Animal Ethics Committee.

Induction of dermatitis by ovalbumin

Mice were sensitized with repeated epicutaneous application of 200µg chicken egg ovalbumin (OVA) (Sigma, Steinheim, Germany) according to a modified previously described method (Nieuwenhuizen et al, 2009). Essentially, a 1-2 cm area of skin on the abdomen of each mouse was shaved and a patch containing PBS or OVA applied overnight (Band-Aid, Johnson & Johnson, Broadway, Australia). Patches were removed for a 2 week rest period following which the entire procedure was repeated twice. Mice were killed 1 week after the final patch and local skin changes were assessed microscopically. Epidermal hyperplasia was quantified (40-60 measurements per mouse) using NIS-elements BR-3 (Nikon, South Africa).

Histology

Skin taken from the site of epicutaneous exposure was preserved in 4% phosphate-buffered formalin at room temperature and embedded in wax. Firstly, Paraffin sections were stained with hematoxylin and eosin for hyperplasia analysis, sirius red for eosinophils (50-60 fields per group at 400x) and toluidine blue for mast cells (10-18 fields per group at 100x). Then p44/42 MAPK (Erk1/2), Phospho-p44/42 MAPK (ERK1/2) (Thr202/Tyr204), c-Jun (60A8) and Phospho-c-Jun (Ser 73) (Cell Signalling, Danvers, MA, USA) followed by DAB staining anti-Rabbit IgG HRP-linked secondary antibody for IL-13Rα2 signalling pathway analysis.

Western Blot Analysis

Lysates from skin sections were prepared in RIPA buffer containing protease inhibitor and quantitated using the BCA™ Protein assay kit (Thermo-Scientific Pierce, Rockford IL, USA). A total of 15μg heat-denatured (95°C) protein was separated via SDS-PAGE and transferred to a nitrocellulose membrane according to conventional protocols. Membranes were blocked in 5% milk in TBS-Tween (TBST) for 1 hour and probed with the following primary antibodies in 5% BSA-TBST at 4°C overnight: Phospho-p44/42 MAPK (ERK1/2) (Thr202/Tyr204) and Phospho-c-Jun (Ser 73) (Cell Signalling, Danvers, MA, USA). After washing with TBST, membranes were incubated with the appropriate secondary antibody for 1 hour at room temperature. Protein levels were visualized by chemiluminescence using the LumiGlo® Reserve Substrate (KPL, Gaithersburg, MA, USA) and the VisionWorks LS Biospectrum™ 500 Imaging System (UVP, Cambridge, UK). For detection of unphosphorylated protein levels, membranes were stripped

with 0.1M glycine-HCl (pH 2.2) and re-probed with the following antibodies: p44/42 MAPK (Erk1/2) and c-Jun (60A8) (Cell Signalling, Danvers, MA, USA), followed by chemiluminescent detection as described above.

Cytokine production by splenocytes and inguinal lymph nodes

Individual spleens or inguinal lymph nodes were collected from ovalbumin treated mice respectively in complete Iscove's Modified Dulbeccos Medium (IMDM) supplemented with; 10% FCS (Gibco, Paisley, Scotland), penicillin, streptomycin, 1mM sodium pyruvate, 50µM B2-ME and NEAA (Sigma Steinheim, Germany). Single cell suspensions were obtained by pressing spleens or lymph nodes through a 70µm cell strainer and centrifugation at 1200rpm for 5min at 4°C in a 15ml tube. The pelleted cells were depleted of red blood cells by hypotonic lysis in Red Cell Lysis Buffer and the centrifugation step was repeated. Cells were resuspended in 2ml complete IMDM and stained with Trypan Blue (Sigma Steinheim, Germany) to count viable cells in a haemocytometer. Cells were diluted to $1x10^6$ cells/ml and cultured in a 96-well plate in complete IMDM with anti-CD3 (clone: 145-2C11, 10µg/ml) for 48h at 37°C and 5% CO_2. Supernatants were collected and stored at -80°C.

Cytokine ELISA

Sandwich ELISAs were performed to determine cytokine levels in cell supernatants. Maxisorp microtitre plates were coated with purified anti-IL-13 (clone: 38213, 1µg/ml, BD Biosciences Pharmingen, San Diego, CA, USA), diluted in phosphate buffered saline (PBS, pH 9.5) and incubated overnight at 4°C. Plates were blocked with milk powder in PBS for 3h at 37°C and

serially diluted standard, purified recombinant IL-13 (BD Biosciences Pharmingen, San Diego, CA, USA) were added. Cell supernatants were added, diluted in ELISA dilution buffer containing bovine serum albumin in PBS and incubated overnight at 4°C. Biotinylated anti-mouse secondary antibodies for γ (clone: XMG1.2) or IL-13 (goat anti-mouse, 0.5μg/ml, BD Biosciences Pharmingen, San Diego, CA, USA) were added for 3h at 37°C followed by HRP labeled streptavidin. Subsequently, plates were incubated with TMB Peroxidase Substrate (KPL, Gaithersburg, MA, USA), the color reaction stopped with 2M H_2SO_4 and absorption measured at 450nm. ELISA wash buffer was used to wash plates 4x between each step.

Total IgE detection by ELISA

Total IgE levels were measured in the serum of ovalbumin-treated mice by sandwich ELISA (as above). Anti-mouse IgE (clone: 84.1C) mAb was used for coating, purified recombinant mouse IgE (BD Biosciences Pharmingen, San Diego, CA, USA) as a standard and alkaline phosphotase-labeled anti-mouse IgE mAb (23G3, Southern Biotechnology, Birmingham, AL, USA) for detection. 4-Nitrophenylphosphate (Fluka, Switzerland) dissolved at 1mg/ml in substrate buffer was added to all samples and the absorbance measured at 405nm.

Histology

Skin taken from the site of epicutaneous exposure was preserved in 4% phosphate-buffered formalin at room temperature and embedded in wax. Sections were stained with p44/42 MAPK (Erk1/2) and Phospho-p44/42 MAPK (ERK1/2) (Thr202/Tyr204) (Cell Signalling, Danvers,

MA, USA) followed by DAB staining anti-Rabbit IgG HRP-linked secondary antibody for IL-13Rα2 signalling pathway analysis.

Western Blot Analysis

Lysates from skin sections were prepared in RIPA buffer containing protease inhibitor and quantitated using the BCA™ Protein assay kit (Thermo-Scientific Pierce, Rockford IL, USA). A total of 15μg heat-denatured (95°C) protein was separated via SDS-PAGE and transferred to a nitrocellulose membrane according to conventional protocols. Membranes were blocked in 5% milk in TBS-Tween (TBST) for 1 hour and probed with the following primary antibodies in 5% BSA-TBST at 4°C overnight: Phospho-p44/42 MAPK (ERK1/2) (Thr202/Tyr204) and Phospho-c-Jun (Ser 73) (Cell Signalling, Danvers, MA, USA). After washing with TBST, membranes were incubated with the appropriate secondary antibody for 1 hour at room temperature. Protein levels were visualized by chemiluminescence using the LumiGlo® Reserve Substrate (KPL, Gaithersburg, MA, USA) and the VisionWorks LS Biospectrum™ 500 Imaging System (UVP, Cambridge, UK). For detection of unphosphorylated protein levels, membranes were stripped with 0.1M glycine-HCl (pH 2.2) and re-probed with the following antibodies: p44/42 MAPK (Erk1/2) and c-Jun (60A8) (Cell Signalling, Danvers, MA, USA), followed by chemiluminescent detection as described above.

Supplementary: References

Emson CL, Bell SE, Jones A, et al. (1998). Interleukin (IL)-4-independent induction of immunoglobulin (Ig)E, and perturbation of T cell development in transgenic mice expressing IL-13. *J Exp Med* 188: 399-404.

McKenzie GJ, Bancroft A, Grencis RK, et al. (1998). A distinct role for interleukin-13 in Th2-cell-mediated immune responses. *Curr Biol* 8: 339-342.

Mohrs M, Ledermann B, Kohler G, et al. (1999). Differences between IL-4- and IL-4 receptor alpha-deficient mice in chronic leishmaniasis reveal a protective role for IL-13 receptor signalling. *J Immunol* 162: 7302-7308.

Noben-Trauth N, Kropf P, Muller I (1996). Susceptibility to Leishmania major infection in interleukin-4-deficient mice. *Science* 271: 987-990.

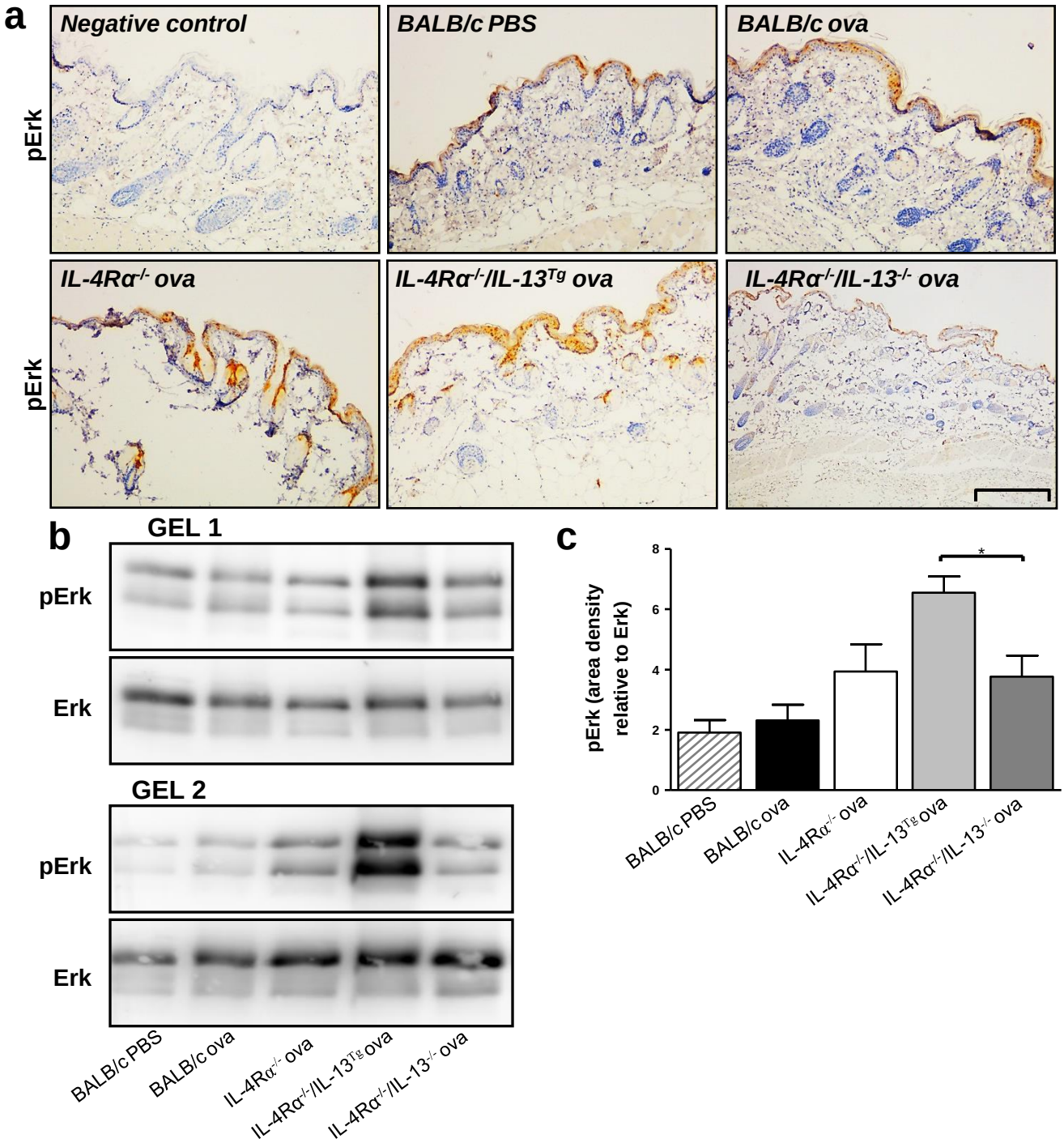

Figure S1: ERK activation during dermatitis

(a) DAB stained phosphorylated ERK 1/2, using phospho-p44/42 MAPK (Thr202/Tyr204) antibodies. **(b)** Western blot comparing ERK 1/2 and phosphorylated ERK 1/2. Pictures show 2 individual experiments (n=3). **(c)** Area density graphs are pooled data from 2 experiments, (n=5-6). *=$p<0.05$ IL-4Rα$^{-/-}$/IL-13^{Tg} vs. IL-4Rα$^{-/-}$/IL-13^{Tg} ova mice. Scale bar = 100µm.